A&A 379, 279–287 (2001)
DOI: 10.1051/0004-6361:20011308

Astronomy & Astrophysics

No planet for HD 166435

D. Queloz[1], G. W. Henry[2], J. P. Sivan[3], S. L. Baliunas[2,4,5], J. L. Beuzit[6], R. A. Donahue[4,5], M. Mayor[1], D. Naef[1], C. Perrier[6], and S. Udry[1]

[1] Observatoire de Genève, 51 Ch. des Maillettes, 1290 Sauverny, Switzerland
e-mail: Didier.Queloz@obs.unige.ch
[2] Center of Excellence in Information Systems, Tennessee State University, 330 10th Avenue North, Nashville, TN 37203, USA
[3] Observatoire de Haute Provence, 04870 Saint-Michel l'Observatoire, France
[4] Harvard-Smithsonian Center for Astrophysics, 60 Garden Street, Cambridge, MA 02138, USA
[5] Mount Wilson Observatory, 740 Holladay Road, Pasadena, CA 91106, USA
[6] Observatoire de Grenoble, 414 rue de la Piscine, 38041 Domaine Universitaire de St Martin d'Hères, France

Received 9 August 2001 / Accepted 20 September 2001

Abstract. The G0 V star HD 166435 has been observed by the fiber-fed spectrograph ELODIE as one of the targets in the large extra-solar planet survey that we are conducting at the Observatory of Haute-Provence. We detected coherent, low-amplitude, radial-velocity variations with a period of 3.7987 days, suggesting a possible close-in planetary companion. Subsequently, we initiated a series of high-precision photometric observations to search for possible planetary transits and an additional series of Ca II H and K observations to measure the level of surface magnetic activity and to look for possible rotational modulation. Surprisingly, we found the star to be photometrically variable and magnetically active. A detailed study of the phase stability of the radial-velocity signal revealed that the radial-velocity variability remains coherent only for durations of about 30 days. Analysis of the time variation of the spectroscopic line profiles using line bisectors revealed a correlation between radial velocity and line-bisector orientation. All of these observations, along with a one-quarter cycle phase shift between the photometric and the radial-velocity variations, are well explained by the presence of dark photospheric spots on HD 166435. We conclude that the radial-velocity variations are not due to gravitational interaction with an orbiting planet but, instead, originate from line-profile changes stemming from star spots on the surface of the star. The quasi-coherence of the radial-velocity signal over more than two years, which allowed a fair fit with a binary model, makes the stability of this star unusual among other active stars. It suggests a stable magnetic field orientation where spots are always generated at about the same location on the surface of the star.

Key words. stars: activity – individual: HD 166435 – planetary systems

1. Introduction

A large extra-solar planet survey has been underway since 1994 at the Observatory of Haute-Provence with the high-precision, fiber-fed echelle spectrograph ELODIE (Baranne et al. 1996) mounted on the 193 cm telescope. The search for extra-solar planets is carried out by seeking changes in the radial velocity of each star produced by gravitational interaction with orbiting planets. In 1995 this program lead to the first detection of an extrasolar planet orbiting a Sun-like star (Mayor & Queloz 1995). Our survey contains 324 G dwarf stars brighter than $V = 7.65$, including HD 166435 (Queloz et al. 1998b).

Send offprint requests to: D. Queloz,
e-mail: queloz@obs.unige.ch

The star HD 166435 is a G0 dwarf with $(B - V) = 0.633$. From its distance of 25 pc and its apparent magnitude $m_V = 6.85$, we find an absolute magnitude $M_V = 4.8$. If the metallicity is roughly solar, HD 166435's location in the H-R diagram suggests a main-sequence age of a few billion years. Interestingly, the star was detected in the ROSAT all-sky survey as an extreme ultraviolet (EUV) source, but no other evidence of activity was found by Mulliss & Bopp (1994) in their analysis of the H_α and CaII (8542 Å) lines. Burleigh et al. (1997) found a hint of emission in the CIV (1549 Å) line but detected no other obvious spectral emission features. When we selected HD 166435 for ELODIE observations, we had no real indication that HD 166435 might be young and active. A possible coincidence with another EUV source had been mentioned (Burleigh et al. 1997) as a possible explanation for the EUV ROSAT detection.

After only a few radial-velocity measurements of HD 166435, it became apparent that the star exhibited low-amplitude, radial-velocity variations with a period of about 4 days. Further measurements in the following months confirmed our initial finding, leading us to believe that HD 166435 may have a planetary companion in a close orbit. Subsequently, we began a campaign of high-precision photometric observations with an automatic photoelectric telescope (APT) at Fairborn Observatory in Arizona to search for planetary transits and made tentative plans to announce the new planet at the Protostars and Planets IV conference (Mannings et al. 2000). To our surprise, however, we found the star to be photometrically variable with the same period as the radial-velocity variations. In this article we describe these data, along with additional Ca II H and K measurements acquired at Mount Wilson Observatory, and discuss the most likely explanation for the observed variations in all three data sets.

2. ELODIE spectra

We obtained 70 spectra with ELODIE from 1997 May to 1999 September. These spectra have typical signal-to-noise ratios of 70–150 (at 5000 Å) per resolution element and a resolution ($\lambda/\Delta\lambda$) of about 42 000. The data reduction was carried out on-line during the observations by the ELODIE automatic reduction software (see Baranne et al. 1996 for details). All the spectra were acquired in the high-precision mode, which provides a simultaneous thorium reference spectrum. The zero-point wavelength calibration has an intrinsic instrumental precision of $10\,\mathrm{m\,s^{-1}}$.

To examine certain key spectral features, we co-added the 70 individual spectra to obtain a composite spectrum with a very high signal-to-noise ratio of about 1000. Since the individual spectra were sampled at slightly different velocities relative to the star due to the earth's orbital motion, the composite spectrum also has a better quality than the individual spectra. Two key spectral features in the composite spectrum are shown in Fig. 1. The Ca II H spectral region shows an emission reversal in the core of the absorption line, suggesting strong chromospheric activity. The broader Ca II photospheric wings compared to the Sun are the consequence of the higher effective temperature of HD 166435. No strong lithium absorption line is seen. The comparison with the Sun's spectrum suggests that, with our resolution, the sensitivity to the ^{7}Li doublet is limited to medium or strong features. Moreover, in the case of HD 166435, the lithium doublet is blended with a nearby feature due to rotational broadening. However, it appears that the ^{7}Li feature in HD 166435 is no stronger than the one in the solar spectrum. We estimate an upper limit of 10 mÅ for the ^{7}Li doublet at 6707.8 Å. The curve of growth from Soderblom et al. (1993a) then implies an upper limit for the lithium abundance of $N(\mathrm{Li}) < 1.7$.

We computed the radial velocity of each individual spectrum with the ELODIE automatic reduction software, which uses a cross-correlation technique with binary mask templates. In addition to the stellar radial velocity, the cross-correlation function (CCF) provides additional information about features in the averaged spectral lines (see Queloz 1994 for a review). The width of the CCF yields the $v \sin i$ of the star, while the equivalent width of the CCF can be used as a metallicity estimate if the temperature of the star is known approximately (Mayor 1980; Benz & Mayor 1981; Queloz 1994). The mean equivalent width of the CCF for the 70 individual spectra is similar to the value measured for the Pleiades stars of the same temperature ($B-V_0 = 0.63$). Therefore, a solar metallicity can be assumed for HD 166435. With the same technique and calibration described in Queloz et al. (1998a), we derive a mean $v \sin i = 7.6 \pm 0.5\,\mathrm{km\,s^{-1}}$. A similar value is measured by CORAVEL ($v \sin i = 7.7 \pm 0.7\,\mathrm{km\,s^{-1}}$).

2.1. Radial-velocity data

Analysis of our entire two-year radial-velocity data set revealed a periodicity of 3.7987(±.0004) days. The radial velocities are shown in Fig. 2 where they are phase folded on that period. We fit these data with a binary model and derived a slight orbital eccentricy $e = 0.2$ and an amplitude $K = 83\,\mathrm{m\,s^{-1}}$, corresponding to a minimum mass for a planetary companion of $0.6\,M_\mathrm{J}$. The rms of the residuals to the fit is $28\,\mathrm{m\,s^{-1}}$. A large value compared to the typical ELODIE precision of $10\,\mathrm{m\,s^{-1}}$. If the binary model is the correct interpretation of the observed radial-velocity variations, then additional radial-velocity scatter intrinsic to the atmosphere of the star must be present.

In order to test the binary hypothesis, we first investigated the coherence time of the radial-velocity variations. Since a short-period planet in a (presumed) circular orbit induces sinusoidal reflex motion in the star, we fit sine curves with a period of 3.7987 days to subsets of the radial-velocity observations of increasing duration and computed the rms of the residuals in each case. The results of this test are shown in Fig. 3. The rms of the sinusoidal fits increase with an increase of the duration of the data sets. For durations less than 30 days, the residuals are in agreement with the expected rms by the photon and instrumental noise. For durations longer than 30 days, phase disruptions likely occur and limit the phase coherence and therefore increase the rms of the fit.

To quantify the phase disruptions in the radial-velocity data, we searched for phase changes among 21-day blocks of data spread over the two-year duration of our observations. From Fig. 3 above, we see that, for data sets of three weeks duration, the radial-velocity variations are coherent enough to be described as a sinusoid to within the precision of the measurements. The top panel of Fig. 4 shows phase shifts of up to ±0.1 cycle among the 21-day blocks of data. For comparison, we applied the same procedure to the 51 Peg radial-velocity data, where the circular orbital

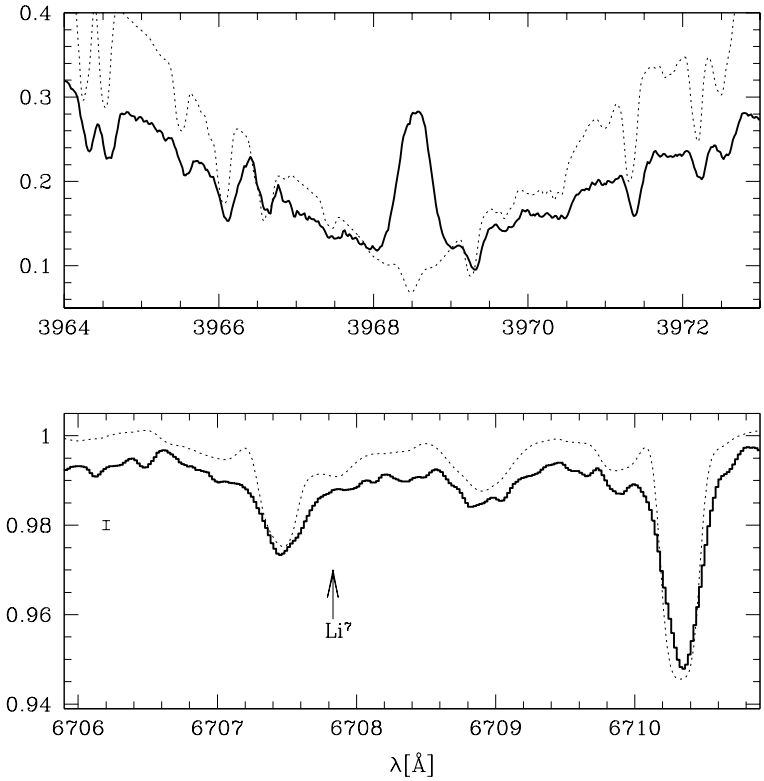

Fig. 1. Selected regions of the composite spectra of HD 166435 (solid line). For comparison, a solar integrated spectrum (Kurucz et al. 1984) with the same resolution has been superimposed (hatched line). Upper panel Ca II H line. An emission feature is clearly visible in the core of the line. Lower panel Region of the Li^7 line at 6708 Å. The solar spectrum is slightly offset upwards for display purpose. No strong Li^7 feature is detected in the HD 166435 spectrum. Notice in both figures the larger line broadening of HD 166435 compared to the Sun.

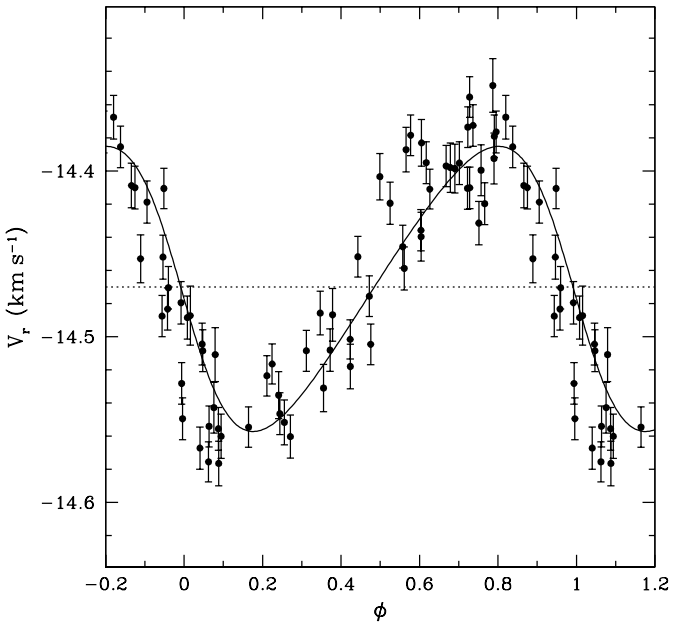

Fig. 2. Phase diagram of the radial-velocity data with a period of 3.7987 day. A binary model is superimposed on the data (solid line). See text for details.

motion of this confirmed planet in close orbit produces sinusoidal reflex motion. As expected, no significant phase changes can be seen in the 51 Peg data (Fig. 4, bottom panel). Interestingly, the random phase changes in the radial velocities from HD 166435, while signifcantly larger than in 51 Peg, are not so large as to prevent their reasonably good description by a sinuosidal model of the whole two-year data set.

The detection of significant phase shifts in the HD 166435 radial velocities explains the high rms ($28\,\mathrm{m\,s^{-1}}$) of the residuals to the planet model fit in Fig. 2. We also examined the amplitude K of the fits and their zero levels V_0 for similar changes with the same technique. No significant change of the K amplitude was detected for either star. The V_0 values for HD 166435 exhibited small variations that are probably related to line-profile variations (see below).

2.2. Line profile and bisector analysis

The radial velocity of a star is defined to be the velocity of the center of mass of the star along our line of sight. However, the observational determination of a star's radial velocity is accomplished by measuring the Doppler shift of spectral lines produced in the stellar atmosphere. If changes occur in the star's spectral-line profiles, the measured Doppler shifts may not correspond precisely to the velocity of the star's center of mass. For pulsating stars

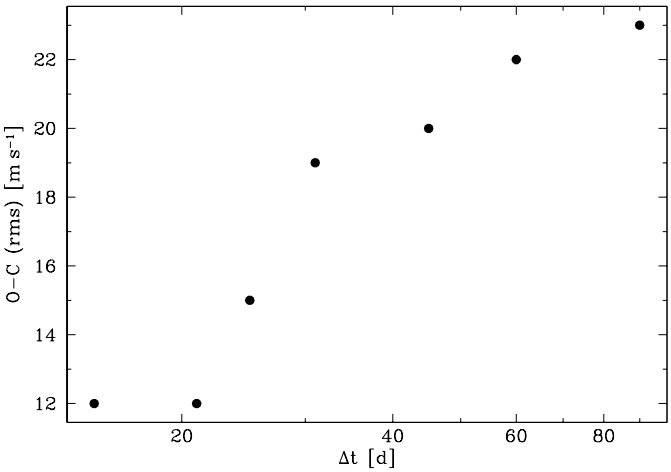

Fig. 3. Variation of the rms (O–C) of a sine-curve fit to the radial-velocity data versus the time duration of the observations.

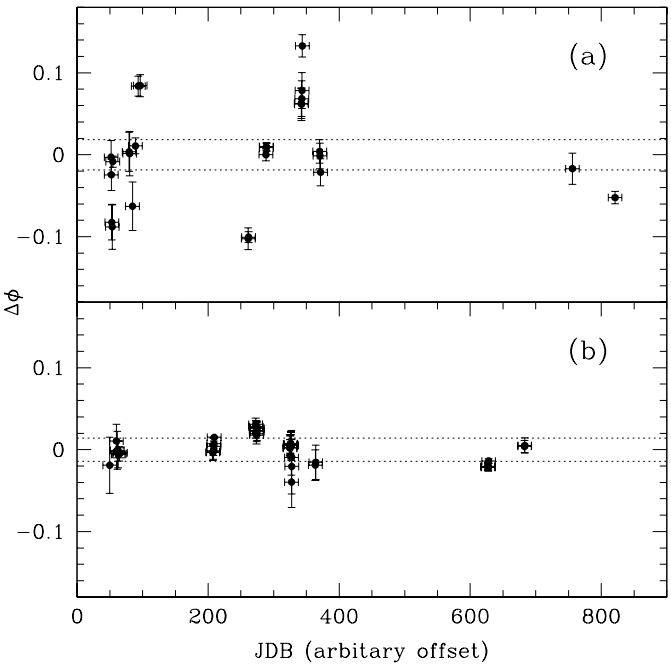

Fig. 4. Phase shifts in the radial velocities derived by fitting sine curves to subsets of the data with a maximum duration of 21 days. **a)** HD 166435 data. **b)** 51 Peg data. Note that there is an arbitrary time offset between the two data sets for display purposes. The two hatched lines in each panel indicate the $\pm 1\sigma$ error on the global fit.

and stars with very active atmospheres, this is indeed the case.

To interpret observed radial-velocity variations as true changes in the velocity of the star, we must show that the observed variations do not stem from changes in the stellar atmosphere. One of the best ways to do this is to look for subtle changes in the line profiles. Radial-velocity changes in a star accompanied by spectral-line profiles that are constant in time would be a direct evidence for real velocity changes in the star's center of mass. The detection of line-profile changes would point instead to atmospheric phenomenon.

The computation of a stellar radial velocity from a particular spectrum with the CCF technique involves the correlation of thousands of spectral lines. Thus, in order for line-profile changes to affect the radial-velocity measurements, the profile changes in a particular spectrum must affect all of the spectral lines in a similar way. Otherwise, no change would be induced in the cross-correlation function.

Our CCF technique employs a binary template (Queloz 1994) and is a very efficient way to look at global phenomena in spectra. The CCF function represents a mean spectral-line profile of all of the lines selected by the template. To study the mean spectral-line profile of HD 166435, we designed a specific template that selects only the weak and non-saturated spectral lines. We used the line-bisector technique to analyze the CCF profiles in the same way that we would analyze an individual spectral line. In Fig. 5 we show HD 166435's mean CCF and its bisector. The bisector displays the classic "C" shape observed in other stars lying on the same (cool) side of the granulation boundary (Gray 1989). Unlike similar studies (Toner & Gray 1988), our data have an absolute wavelength calibration with an accuracy of approximately $10\,\mathrm{m\,s^{-1}}$ (the precision of the instrument). Therefore, we don't need to shift the bisector arbitrarily to a mean value for comparison. Moreover, if a bisector change is detected, we know whether it is the top or the bottom of the bisector that is moving.

We selected two regions of the bisector at the top and bottom of the profile ($\overline{V_\mathrm{t}}$ and $\overline{V_\mathrm{b}}$) (see Fig. 5 for illustration) to measure possible bisector orientation changes with high accuracy. The difference between $\overline{V_\mathrm{t}}$ and $\overline{V_\mathrm{b}}$ is equivalent to the "bisector velocity span" widely used in similar studies (see Toner & Gray 1988). This is actually a measurement of the inverse of the mean slope of the bisector.

Any correlation between radial-velocity changes and line-bisector orientation would cast serious doubts on the reflex-motion interpretation of the radial-velocity variations. If the radial-velocity variations are due to center-of-mass velocity changes of the star, we would see the bisectors oscillating to the left and right of the mean bisector with no change in shape or orientation. In order to investigate this, we first looked at the bisectors of each individual CCF. In Fig. 6 the bisectors of the CCFs for two sets of spectra selected at opposite phases of the radial-velocity cycle ($\phi = 0.0 \pm 0.1$ and $\phi = 0.5 \pm 0.1$) are displayed. Comparison with the mean bisector shows that the bisectors are twisting around the mean bisector with the same periodicity as the radial-velocity signal. The top of the CCF profile moves very little, while the bottom shifts back and forth with an amplitude 50% larger than the K amplitude of the radial-velocity signal. The only way to understand this twisting motion of the bisectors is through a change in the spectral-line profiles synchronized

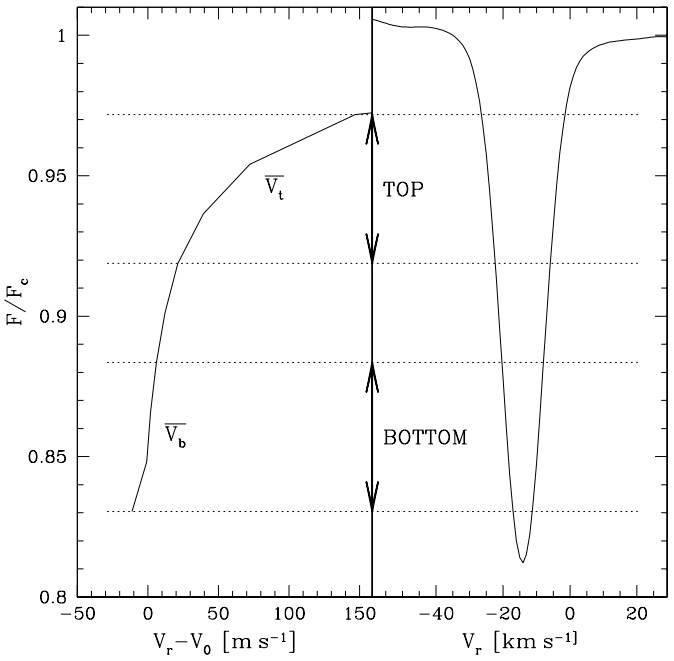

Fig. 5. Right: the mean CCF function of HD 166435's spectra constructed with a template selecting only the weak and non-saturated lines. This profile represents the mean spectral-line profile of the lines selected by the template. Left: the bisector of the CCF. V_0 is an arbitrary offset. Note the definition of the boundaries for the computation of ($\overline{V_t}$ and $\overline{V_b}$).

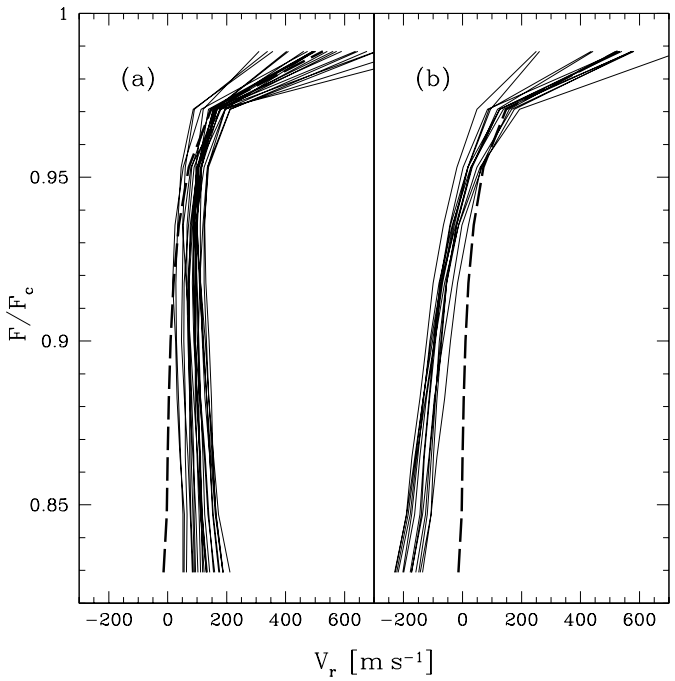

Fig. 6. Individual bisectors for two sets of spectra selected at opposite phases of the radial-velocity cycle. **a)** Spectra measured at $\phi = 0.0 \pm 0.1$. **b)** Spectra measured at $\phi = 0.5 \pm 0.1$. The hatched line illustrates the mean bisector computed by averaging all spectra.

with the radial-velocity cycle. The amplitude of this effect is enough to produce the observed radial-velocity signal.

To investigate further the exact relationship between the orientation of the bisectors (bisector span) and the radial velocity of the CCF, we plot these two parameters in Fig. 7. A direct relationship between the two quantities is clearly visible. A linear solution $(\overline{V_t} - \overline{V_b}) = -0.88(\pm 0.04)V_r$ can be fit with a $27\,\mathrm{m\,s^{-1}}$ rms. Thus, the results of our line-profile analysis of HD 166435's CCFs provide strong evidence that the radial-velocity variations originate in the stellar atmosphere and not from reflex motion of the whole star.

3. Photometry

The *Hipparcos* catalogue lists 144 photometric measurements of HD 166435 acquired between 1990 January and 1993 March and identifies the star as an "unsolved" variable with a range of 0.05 mag (Perryman et al. 1997). Our periodogram analysis of the *Hipparcos* photometry confirms the lack of periodicity, particularly near the radial-velocity period. This is what led us initially to suspect that our observed radial-velocity variations might be due to the presence of a planet in an orbit similar to that of the companion of 51 Pegasi (Mayor & Queloz 1995).

Thus, shortly after the detection of the periodicity in the radial-velocity signal, we began photometric observations of HD 166435 with the T8 0.80 m automatic photoelectric telescope (APT) at Fairborn Observatory in Arizona to search for possible transits of the companion across the disk of the star. We acquired 326 Strömgren b and y observations with a two-channel precision photometer on the APT between 1998 June and 2000 June. The observations were reduced differentially with respect to the comparison star 99 Her (HR 6775, HD 165908, F7V), corrected for atmospheric extinction with nightly extinction coefficients, and transformed to the Strömgren system. External precision of a single observation with the 0.80 m APT averages 0.0011 mag. Further details of the automatic-telescope operations and data-reduction procedures can be found in Henry (1999). The individual photometric observations are available on the Tennessee State University Automated Astronomy Group web site[1].

Periodogram analysis of the entire set of 326 observations taken together reveals a photometric period of 3.7995 ± 0.0005 d. Thus, the photometric and radial-velocity periods agree within their respective uncertainties.

For our photometric analysis we adopt, as reference, the radial-velocity period of 3.7987-day and $T_0 = 2\,450\,996.5$, the radial-velocity maximum of the best-fit sine-curve model. The photometric observations are divided into five groups as shown in Table 1, where we give the results of least-squares, sine-curve fits on the radial-velocity period to the five Strömgren y data sets. We also list the periods derived from the five individual data

[1] `http://schwab.tsuniv.edu/t8/hd166435/hd166435.html`

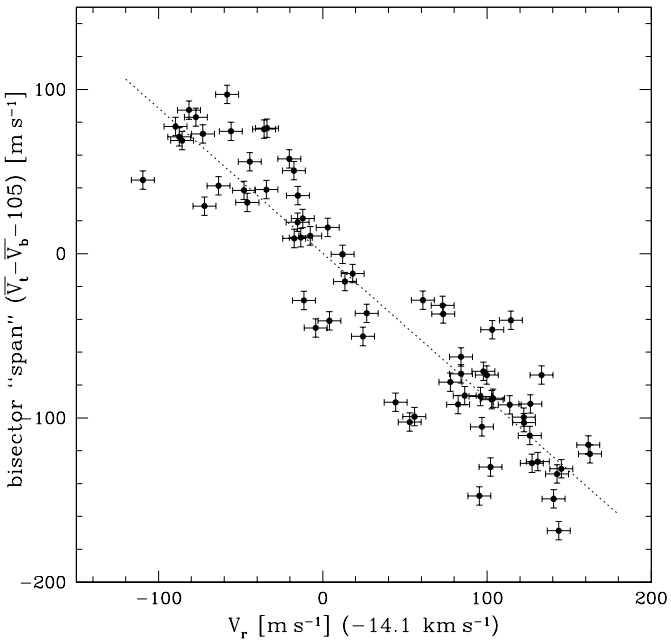

Fig. 7. Radial velocity of each CCF versus the bisector span ($\overline{V_t} - \overline{V_b}$) of the CCF profile. The dotted line is the best linear fit to the data.

sets. The photometric amplitudes vary from 0.050 mag to 0.035 mag; the mean magnitudes of the five data sets have a range of about 0.023 mag. Although the five light curves approximate sinusoids, the rms values are, nevertheless, somewhat higher than the 0.0011 mag precision of typical observations. This is primarily the effect of slight cycle-to-cycle changes in the light curves within each data set; the rms values increase for the later data sets since the later data sets are longer and contain more cycles.

Data set 1, which covers only 10 days or 2.7 cycles, has the largest number of observations since at this time we were making repeated measurements each night to search for transits. These data are plotted in the left and right third panels from the top of Fig. 8. Based on the *Hipparcos* photometry mentioned above, we did not expect to find coherent light variability on this period. Instead, we found a smoothly varying, nearly sinusoidal light curve with a period matching the radial-velocity period and a minimum near phase 0.25, where we had hoped to find transits.

In Fig. 8 we see that the time of radial-velocity maximum, i.e., maximum red shift at phase 0.0, corresponds closely to the time when the light curve crosses its mean level at $\Delta y = 1.85$ mag in the downward direction. The time of photometric minimum corresponds closely to the time when the radial-velocity curve crosses its mean level (zero velocity shift with respect to the mean velocity) in the downward direction. The time of radial-velocity minimum corresponds closely to the time when the light curve crosses its mean level in an upward direction. Finally, the light-curve maximum corresponds closely to the time when the radial-velocity curve crosses its mean level in an upward direction. Hence, these two nearly sinusoidal curves are one-quarter cycle out of phase with each other.

Our Strömgren photometry and $\Delta(b-y)$ colors from data set 1 are plotted in the bottom two panels of Fig. 8, also with phases computed from the radial-velocity ephemeris. The color curve is exactly in phase with the light curve and has a peak-to-peak amplitude of 0.009 mag. The star is redder when it is fainter.

4. Ca II H and K spectrophotometry

From 1998 June to 1998 August, 141 Ca II H and K measurements were made on 20 nights with the 100-inch telescope at Mount Wilson Observatory as part of the HK Project (Baliunas et al. 1998). In that program, measurements of the Ca II H and K lines of several thousand stars are made as a proxy for surface magnetism.

The observed quantity, S, is the flux measured in two 0.1 nm pass bands centered on the H and K lines normalized by two 2.0 nm-wide sections of photospheric flux centered at 390.1 nm and 400.1 nm. A nightly calibration factor is determined from measurements of a standard lamp and standard stars (Baliunas et al. 1995). The night-to-night rms precision of the lamp is on the order of 0.5%, while the standard stars have an average standard deviation of ∼1.5%, which limits the lowest amplitude of variability that can be detected to approximately 1%.

Our periodogram analysis of the 141 Ca II observations over a period range of two to ten days gives a strong periodicity at 3.85 ± 0.01 d, essentially identical to the radial-velocity and photometric periods. Since the time span of the Ca II observations is only 62 days and the period uncertainty is larger than for the radial velocities, we adopted the radial-velocity period and $T_0 = 2\,450\,996.5$ for the analysis.

A 30-day subset of the S measurements, during which we had simultaneous photometry and radial-velocity data, is plotted in the second from the top panels of Fig. 8. A sinusoidal fit to these S values gives an amplitude of 0.023 and a mean value of 0.46. Interestingly, the phase is shifted 1/8 of a cycle compared to the light and color curves (with 15% statistical error). The variation of S is therefore 1/8 cycle out of phase with the radial-velocity variation. The star has its higher level of Ca II H and K emission 1/8 of a cycle after it is faintest and 1/8 of a cycle before it reaches its most red-shifted radial velocity. Similar phase differences between photometric and photospheric data are also detected in the G0 Hyades star VB 31 (Radick et al. 1987).

5. Discussion and modeling

Our observations of HD 166435 indicate that the star is active and thus young. The relatively fast rotation also indicates a young star. If we assume that the X-ray flux detected by ROSAT (Burleigh et al. 1997) indeed originates from the star, the 0.5 c/s PSPC counts in the 0.1–2.4 keV range (Randich & Schmitt 1995) corresponds to $\log(L_X) = 29.5$ or $\log(L_X/L_{bol}) = -4.1$. About the same X-ray luminosity is measured in other single stars

Table 1. Summary of the Strömgren y photometric results.

Data Set	Date Range (JD–2400000)	N_{obs}	Period (days)	Mean Brightness (mag)	Full Amplitude (mag)	Phase of Minimum	rms (mag)
1	50986–50996	219	3.732(6)	1.849(1)	0.050(1)	0.20(1)	0.003
2	51086–51136	16	3.776(7)	1.865(1)	0.052(4)	0.12(1)	0.004
3	51224–51360	42	3.807(10)	1.857(1)	0.025(4)	0.07(3)	0.008
4	51434–51501	25	3.763(34)	1.842(2)	0.023(4)	0.23(3)	0.007
5	51591–51710	24	3.821(7)	1.842(2)	0.032(6)	0.29(3)	0.008

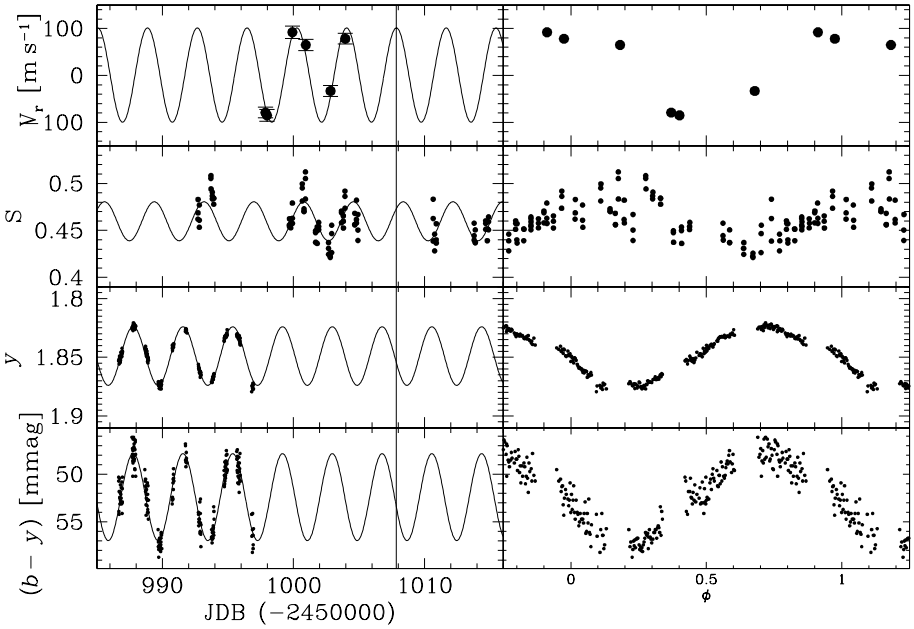

Fig. 8. Left: simultaneous observations of (from the top) radial velocity, S index, delta y magnitude, and delta $(b-y)$ color, of HD 166435 over a time span of 30 days. A best-fit sine-curve with a period fixed at 3.798 days is shown. A vertical line is drawn at an epoch of maximum radial velocity to help visualize the phase offsets between data sets. Right: same data but phase folded with $P = 3.798$ d and $T_0 = 2\,450\,996.5$.

of similar temperature in the 220 Myr cluster NGC 6475 (James & Jeffries 1997). Thus, we estimage the age of HD 166435 to be about 200 Myr.

The typical Li content of G0 stars in the Pleiades is about $\log(N_{\rm Li}) \approx 3.0$. At the age of the Hyades (400 Myr), the lithium is depleted to about 2.6. The solar value is 1.0. The weak lithium content of HD 166435 noted above ($\log(N_{\rm Li}) < 1.7$) conflicts with its young age deduced from its rotation rate and activity level. We have no explanation for this. However, other young stars with low lithium content have been detected in Preasepe (KW 392) (Soderblom et al. 1993b) and Hyades (vB 9, vB 143) (Thorburn et al. 1993).

The brightness of HD 166435, its spectroscopic line profiles, and its chromospheric emission all vary with the 3.8-day periodicity found in the radial velocities. As seen in Fig. 8 above, the brightness variations exhibit a roughly one-quater phase shift with respect to the radial velocities. All of this strongly suggests that the radial-velocity variations are due to the observed stellar activity. For a magnetically active star with dark spots being carried into and out of view by rotation, we would expect to see such a phase shift between the brightness changes and radial-velocity variations. When the spot lies on the central meridian of the star, it lies partly on the approaching and partly on the receeding halves of the stellar disk. The spot also causes the maximum depression in the brightness of the star at this time. Hence the radial-velocity effect of the spot at photometric minimum should be null. As can be seen in Fig. 8 above, the radial-velocity shift is very close to zero at the minimum of the light curve. Radial-velocity minimum (the time of maximum blue shift) should occur as the dark spot approaches the receeding limb of the star and hence is moving out of view. This results in more light from the approaching half of the stellar disk reaching our telescopes than from the spotted, receeding half of the disk. This is in agreement with Fig. 8, where we see that radial-velocity minimum corresponds to a time when the star is rapidly brightening. Similar reasoning predicts that radial-velocity maximum should occur when the star is rapidly dimming, as also observed in Fig. 8. The delta $(b-y)$ color curve in the bottom panel of the figure shows

that the star is redder when it is fainter, further showing that the spots causing the brightness variation must be cooler (darker) than the surrounding photosphere.

The small phase shift between the brightness of HD 166435 and its chromospheric emission level suggests that the photocenter of the dark spot distribution is somewhat offset from the photocenter of the bright plage area. This phenomena is observed on the Sun to a lesser degree where leader spots tend to be larger and to live longer than follower spots, resulting in a displacement up to 5^0 between the photocenters of the spot and the associated plages (Dobson-Hockey & Radick 1986). The larger displacement in HD 166435 suggests that the size of active regions is much larger than those seen on the Sun, in agreement with the observed amplitude of the light curve.

The growth and decay of individual spots on time scales longer than a stellar rotation will affect the phase and amplitude of the radial-velocity signal (as well as the brightness and chromospheric emission levels) on long time scales. Our detection of coherent radial-velocity variations without noticeable phase shifts over intervals of up to 21 days suggests that the spots are stable for at least this long. This provides an estimate of the evolutionary time scale for individual spots of roughly a month. However, we observed a quasi-coherent signal for the entire two-year span of our radial-velocity measurements. This suggests that new spot formation occurs at about the same longitude on the surface of the star during this time. Among the numerous active stars measured in our extrasolar planet survey, the stability of the radial-velocity signal of HD 166435 is unique. None of the other active stars in our sample display the level of phase coherence observed in HD 166435 that could suggest the possibility of planetary reflex motion. Therefore, the spot generation mechanism of HD 166435 may be the result of unusual stability in the geometry of its magnetic field. This phenomenon is not unique amongst active stars. Toner & Gray (1988) observed a stable phase lasting for at least 3 years in the variation of the line bisector of the young star χ Boo A. Stable active regions at the same longitude are observed as well in RS CVs binaries (Jetsu 1996). Moreover, on the Sun, during flares, hot spots have been seen for 30 years at the same longitude (Bai 1988; Bai 1990)

We conclude from these qualitative arguments that a rotating spot model can successfully explain the variability in our spectroscopic and photometric data sets. Moreover, the mean level of the Ca index, $< S >= 0.46$, corresponding to $R'_{\rm HK} = -4.26$, is in a good agreement with the activity level expected for a star with rotation period of 3.8 days (Noyes et al. 1984).

The combination of our rotation period and $v \sin i$ measurements allows us to estimate that the inclination of the star's rotation axis to our line of sight is approximately $i = 30°$. Notice that in our case the increase of the macroturbulence with the star rotation is negligible. It does not change our estimate of the i angle. The smooth (i.e., without plateaus) variations in our radial velocities, photometry, and chromospheric emission suggest that the largest spotted region is always visible to the observer and does not completely disappear when on the far side of the star. Therefore, it is likely that the spot region is located within 30 degrees of the stellar pole and is visible, at least in part, throughout the rotation cycle. In this case, projection effects would be responsible for most of the rotational modulation of the star's brightness.

Thus, we have shown that surface magnetic activity on the star HD 166435 can mimic the kind of radial-velocity variations observed in stars with true planetary reflex motions. However, further analysis of the spectroscopic line profiles, photometry, and chromospheric emission clearly demonstrates that stellar activity is the origin of the radial-velocity variations. Our observations of this peculiar object actually strengthen the interpretation of other low-mass companions to solar-type stars where a low-amplitude, radial-velocity variation has been detected but where photometric, chromospheric, and line-profile variations are absent (e.g., Henry et al. 2000).

Acknowledgements. This work has been made possible thanks to the continuous support from the Fond National de la Recherche Suisse (FNRS) and the efforts made by the telescope staff of the Observatoire de Haute-Provence. We thanks Nuno Santos and Claudio Melo for their contributions on the discussion of the stellar activity.

We are grateful for the efforts of Lou Boyd and Don Epand at Fairborn Observatory. Astronomy with automated telescopes at Tennessee State University is supported through NASA grants NCC5–96 and NCC5–511 and NSF grant HRD–9706268. GWH acknowledges additional support from the Richard Lounsbery Foundation.

The HK Project at Mount Wilson Observatory has been supported by the Richard Lounsbery Foundation, the Scholarly Studies Program and the James Arthur Funds of the Smithsonian Institution, The Olin Wilson Fund of the Mount Wilson Institute, MIT Space Grants # 5700000633 and 7A06, NASA Grant NAG5–7635, and several generous individuals. We are indebted to M. Bradford and K. Palmer for their dedication to the HK Project at Mount Wilson Observatory, which is operated under agreement with the Carnegie Institution of Washington.

References

Bai, T., ApJ, 328, 860
Bai, T., ApJ, 364, L17
Baliunas, S. L., Donahue, R. A., Soon, W., & Henry, G. W. 1998, in The 10th Cambridge Workshop on Cool Stars, Stellar Systems, and the Sun, ed. R. A. Donahue, & J. A. Bookbinder (San Francisco: ASP) ASP Conf. Ser., 154, 153
Baliunas, S. L., Donahue, R. A., Soon, W. H, et al. 1995, ApJ, 438, 269
Baranne, A., Queloz, D., & Mayor, M., et al. 1996, A&AS, 119, 1
Benz, W., & Mayor, M. 1981, A&A, 93, 235
Burleigh, M. R., Barstow, M. A., & Fleming, T. A. 1997, MNRAS, 287, 381
Dobson-Hockey, A. K., & Radick, R. R. 1986, Lect. Notes Phys. 254, ed. M. Zeilik, & D. M. Gibson, 202

Gray, D. F. 1989, PASP, 101, 832
Henry, G. W. 1999, PASP, 111, 845
Henry, G. W., Baliunas, S. L., Donahue, R. A., Fekel, F. C., & Soon, W. 2000, ApJ, 531, 415
James, D. J., & Jeffries, R. D. 1997, MNRAS, 291, 252
Jetsu, L. 1996, A&A, 314, 153
Kurucz, R. L., Furenlid, I., & Brault, J. 1984, National Solar Observatory Atlas, No. 1
Mannings, V., Boss, A. P., & Russell, S. S. 2000, Protostars and Planets IV (Tucson: University of Arizona Press)
Mayor, M. 1980, A&A, 87, L1
Mayor, M., & Queloz, D. 1995, Nature, 378, 355
Mulliss, C. L., & Bopp, B. 1994, PASP, 106, 822
Noyes, R. W., Hartmann, L. W., Baliunas, S. L., Duncan, D. K., & Vaughan, A. H. 1984, ApJ, 279, 763
Perryman, M. A. C., Lindegren, L., Kovalevsky, J., et al. 1997, A&A, 323, 49
Queloz, D. 1994, in New Developments in Array Technology and Applications, ed. A. G. Davis Philip, IAU, 167, 221
Queloz, D., Allain, S., Mermillod, J.-C., Bouvier, J., & Mayor, M. 1998, A&A, 335, 183
Queloz, D., Mayor, M., Sivan, et al. 1998, in Brown Dwrafs and Extrasolar Planets, ed. R. Rebolo, E. L. Martin, & M. R. Zapatero Osorio, ASP Conf. Ser., 134, 324
Radick, R. R., Thompson, D. T., Lockwood, G. W., Duncan, D. K., & Baggett, W. E. 1987, ApJ, 321, 459
Randich, S., & Schmitt, J. H. M. M. 1995, A&A, 298, 115
Soderblom, D. R., Jones, B. F., Balachandran, S., et al. 1993a, AJ, 106, 1059
Soderblom, D. R., Fedele, S. B., Jones, B. F., Stauffer, J. R., & Prosser, C. F. 1993b, AJ, 106, 1080
Thorburn, J. A., Hobbs, L. M., Delyannis, C. P., & Pinsonneault, M. H. 1993, ApJ, 415, 150
Toner, C. G., & Gray, D. F. 1988, ApJ, 334, 1008